Soft Matter

Accepted Manuscript

ROYAL SOCIETY OF CHEMISTRY

www.rsc.org/softmatter

Graphical Abstract

Dynamics on Layer-by-Layer Assembly of Poly(acrylic acid)-Lanthanide Complex Colloid and Poly(diallyldimethyl ammonium)

Jiali Xu[1], Zhiliang Wang[1], Lingang Wen[1], Xianju Zhou[2], Jian Xu[3], Shuguang Yang[*1]

[1]*State Key Laboratory for Modification of Chemical Fibers and Polymer Materials, College of Material Science and Engineering, Donghua University, Shanghai 201620*

[2]*Department of Mathematics and Physics, Chongqing University of Posts and Telecommunications, Chongqing 400065*

[3]*Laboratory of Polymer Physics and Chemistry, Institute of Chemistry, Chinese Academy of Sciences, Beijing 100190*

[*] To whom correspondence should be addressed: shgyang@dhu.edu.cn

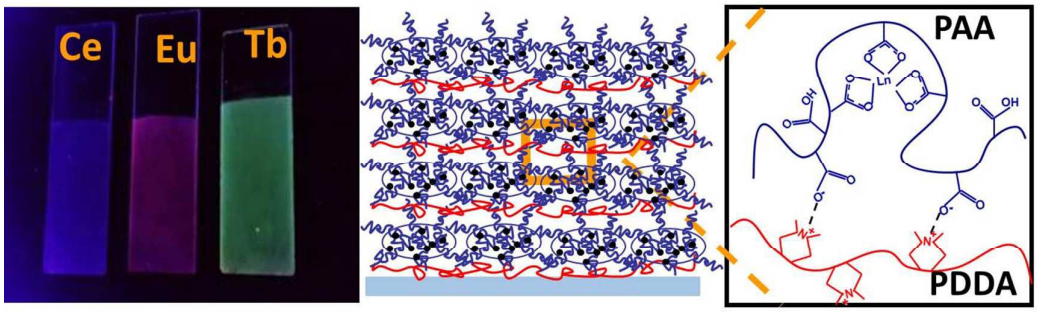

PAA-Ln complex particles and PDDA are assembled and fluorescent films present

Dynamics on Layer-by-Layer Assembly of Poly(acrylic acid)-Lanthanide Complex Colloid and Poly(diallyldimethyl ammonium)

Jiali Xu[1], Zhiliang Wang[1], Lingang Wen[1], Xianju Zhou[2], Jian Xu[3], Shuguang Yang[*1]

[1]*State Key Laboratory for Modification of Chemical Fibers and Polymer Materials, College of Material Science and Engineering, Donghua University, Shanghai 201620*

[2]*Department of Mathematics and Physics, Chongqing University of Posts and Telecommunications, Chongqing 400065*

[3]*Laboratory of Polymer Physics and Chemistry, Institute of Chemistry, Chinese Academy of Sciences, Beijing 100190*

[*] To whom correspondence should be addressed: shgyang@dhu.edu.cn

Abstract

Poly(acrylic acid) (PAA) and lanthanide (Ln) ions, such as Ce^{3+}, Eu^{3+} and Tb^{3+}, were prepared into dispersed complex colloidal particles through three different protocols with rigorously controlling pH value and mixing ratio. The negatively charged PAA-Ln complex particles were layer-by-layer (LbL) assembled with positively charged poly(diallyldimethyl ammonium) (PDDA) to prepare a thin film. The film thickness growth is much quicker than PDDA/PAA film. Due to the incorporation of Ln^{3+} ion, the film exhibits fluorescence. During LbL assembly, PDDA-PAA association based on electrostatic force and PAA-Ce association based on coordination have competition, which leads LbL assembly of PDDA and PAA-Ln complex colloidal particles to be a complicated dynamic process.

Introduction

Layer-by-layer (LbL) assembly, introduced by Decher and coworkers at early 1990s, has been developed into a versatile method to prepare films, coatings and microcapsules with fine-tuned structure.[1-8] Various species such as synthetic polymers, proteins, polysaccharides, dendrimers, inorganic nano-particles and viruses have been utilized for LbL assembly.[9-15]

Recently, polymeric complexes are also used as building block for LbL assembly.[16-19] Polymeric complex is a kind of supramolecular aggregates basing on different secondary interactions, which includes polymer-polymer complex, polymer-surfactant complex, and polymer-metal complex. [20] Compared with simple polymers, polymeric complexes have hierarchical structure, large dimensional size, and multi-compositions. LbL assembly of polymeric complexes is easy to fabricate micrometer thick film and incorporate more components into the film, which is favorable for realizing different functionalities, such as super-hydrophobic, self-healing, and electrochromism .[21-23]

Negatively charged polyelectrolyte complex of poly(acrylic acid) (PAA) and diazoresin (DAR) and positively charged polyelectrolyte complex of poly(styrene sulfonate) (PSS) and DAR were LbL assembled, and the film thickness exceeded 2 μm after 20 dipping cycles.[24] The hydrogen-bonded complex of poly(vinyl pyrrolidone) and PAA (PVPON-PAA) was alternately deposited with poly(methacrylic acid) (PMAA), and the film exhibited exponential thickness growth.[25] PAA complexed with cetyltrimethylammonium (CATB) micelle as a building block was assembled with a cationic polyelectrolyte poly(diallyldimethylammonium) (PDDA).[26] Polymer-metal complexes, with enormous potential by improving the capacity of polymer structural material, have also been utilized for LbL assembly.[27-33] PAA partially complexed with metal ions and PAH were alternately deposited on different substrates to prepare thin films.[30-32] Poly(ethyleneimine) (PEI) and Ag^+ ions can form complex basing on coordination. Bruening et al. reported LbL assembly of PEI-Ag complex nano-particles and PAA.[33]

Generally, polymeric complex precipitates out from the solution and the solid deposition is formed. To fit LbL assembly, polymeric complex needs to be prepared as the form of colloidal particles. Polymer complex colloidal particles are soft and flexible. The dynamic of LbL assembly of polymer complex colloidal particles is an interesting process, but up to now it has rarely been investigated. In this work, we study LbL assembly behaviors of a kind of polymer-metal (PAA-Ln) complex colloidal particles. We adopt three different protocols to prepare negatively charged PAA-Ln complex colloidal particles. PAA-Ln complex colloidal particles are LbL assembled with PDDA to fabricate a composite thin film. We investigate the film growth and discuss dynamics of the LbL assembly. Lanthanides, showing characteristic properties on optics, electrics and magnetics, [34, 35] are incorporated into the film through PAA-Ln complex colloidal particles, and hence the film is endowed with properties of lanthanides, which will show potential applications, such as luminescence or catalysis.

Experimental

Materials

Poly(acrylic acid) (PAA, sodium salt, $M_w \sim 15\ 000$, 35 wt % solution) and poly(diallyldimethylammonium chloride) (PDDA, 20 wt % in water, $M_w \sim 150\ 000$) were bought from Sigma-Aldrich. Cerium chloride heptahydrate ($CeCl_3 \cdot 7H_2O$), terbium chloride hexahydrate ($TbCl_3 \cdot 6H_2O$) and europium chloride hexahydrate ($EuCl_3 \cdot 6H_2O$) were provided by Aladdin, Alfa Aesar, and J&K Chemical, respectively. Sulfuric acid (H_2SO_4, 98 %) and hydrochloric acid (HCl, 36 %) were purchased from Ping Hu chemical. Hydrogen peroxide (H_2O_2) was bought from Sino Pharm Chemical Reagent. Sodium hydroxide (NaOH) was from Shanghai Ling Feng Chemical Reagent. All chemicals were used as received without further purification.

Preparation of PAA-Ln Complex Colloidal Particles

PAA and $CeCl_3 \cdot 7H_2O$ were dissolved in deionized (DI) water. The pH values of

solutions were adjusted to 6.0 using HCl solution or NaOH solution with monitoring of a pH-meter (Mettler, SR-40). The concentration of Ce^{3+} ions was fixed at 0.02 mol/L. PAA concentrations (with respect to the repeating unit [AA]) increased from 0.02 mol/L to 0.2 mol/L. PAA-Ce complexes were prepared by mixing PAA solution and Ce^{3+} solution with the same volume.

At the molar ratio ([AA]/[Ce]) of 10.0, there are three protocols to prepare PAA-Ce complex colloid particle: (1) Ce^{3+} solution and PAA solution were mixed directly; (2) Ce^{3+} solution was drop-wise added into PAA solution at the rate of 1.0 mL/h; (3) PAA solution was drop-wise added into Ce^{3+} solution at the rate of 1.0 mL/h. The preparation of PAA-Eu or PAA-Tb complex colloidal particles is the same as that of PAA-Ce complex.

Thin Film Fabrication

Thin films were prepared *via* LbL assembly of PDDA and PAA-Ln complex colloidal particles. Quartz and silicon slides were (1.2 cm×4.5 cm) used as substrates and thoroughly cleaned by piranha solution (H_2SO_4 and H_2O_2 mixture, 7/3 v/v) for 30 min before use, followed by rinsing with DI water and finally drying with pure nitrogen flow. The LbL assembly was conducted with an automatic dipping machine (Kejing Auto Instrument, Shenyang). The machine can be programmed to immerse the substrates into different solutions for different times. The substrate was alternately immersed in PDDA solution and PAA-Ln complex nano-particle solution, with the interval of three rinses in water. The assembling and rinsing time was set to 4 and 1 min, respectively. The prepared film is expressed as $[PDDA/(PAA@Ln)]_n$, where the subscript *n* indicates that the film was fabricated through *n* assembling cycles. The symbol @ means that lanthanide ion is buried in the complex colloidal particle.

Characterization

Dynamic laser light scattering (DLS) of PAA-Ln complex was conducted with the system from Brookhaven Instruments Corporation (BI-200SM Goniometer; laser: 40 mW, λ = 532 nm). Zeta Potential measurement was recorded using Mastersizer Instruments Zetasizer 200 (Malvern UK), equipped with a 4 mV He-Ne laser (632.8 nm). A Nanocalc-XR (Ocean Optics, Germany) optical instrument was used to

measure the near-normal reflection spectra of the thin films deposited on silicon wafers, and the film thickness was calculated based on refection spectra. X-Ray photoelectron spectroscopy (XPS) analysis was performed on the Thermo Scientific ESCALab 250Xi using 200 W monochromated Al Kα radiation. The fluorescence spectra were recorded at room temperature with Shimadzu 5301-RF machine.

FT-IR characterization was performed on a Nicolet 8700 spectrophotometer with a spectral resolution of 4 cm^{-1}. PAA solution at pH 6.0 was frozen-dried to get the solid sample. PAA solution and PDDA solution were mixed at pH 6.0, and then centrifuged to get the polymer complex bulk. PAA and PDDA/PAA bulk samples were all dried in vacuum at 40 ℃ for 24 h and then pressed into standard KBr discs for IR characterization. $[PDDA/(PAA@Ce)]_{20}$ thin film deposited on the silica substrate was measured by IR spectrometer directly with blank silicon wafer as background. The content of cerium in the film was measured using inductively coupled plasma atomic emission spectroscopy (ICP-AES) (Prodigy, Leeman, US).

Quartz crystal microbalance (QCM) and the chips were provided by Suzhou Institute of Nano-Tech and Nano-Bionics. The resonance frequencies were monitored at the third overtone number. PDDA solution and PAA-Ce complex nano-particle solution were both diluted 10 times and alternately pumped through the chamber for 15 min at the rate of 40 μL/min. During the switching of the assembling solution, water was sent through for 10 min to rinse the chip in the chamber also at the rate of 40 μL/min.

Results and discussions

Preparation of dispersed PAA-Ln Complex Colloidal Particles

Basing on coordination, PAA and Ln^{3+} ions can form polymer-metal complex.[36-38] The carboxylic acid groups (COOH) show much weaker interaction with lanthanide ion than the ionized carboxylate groups (COO^-). So the formation of PAA-Ln complex shows strong dependence on pH value.[38] At pH values below 2.5, the polymer-metal complex is hard to form due to the protonation of carboxylate.

When mixing PAA and Ln^{3+} ion solution at pH values above 2.5, the solution becomes turbid, indicating the formation of PAA-Ln complex. [38] But when pH is higher than 7.5, $Ln(OH)_3$ precipitation cannot be avoided. [38] So the suitable pH region for PAA-Ln complex formation is from 2.5 to 7.5. In this work, PAA solution and lanthanide ion solution were both adjusted to pH 6.0, and PAA-Ln complex were prepared by mixing PAA and lanthanide solutions.

Generally, PAA-Ln complex precipitates out from solution quickly. Different mixing molar ratios ([AA]/[Ce]) were tried to prepare dispersed PAA-Ce complex colloidal particles. As shown in Figure 1 when the molar ratio changes, the solutions will show different turbidity. At the molar ratio from 1.0 to 6.0, the solution turbidity increases. At the molar ratio of 6.0, the solution exhibits the highest turbidity. Further increasing the ratio, the solution turbidity decreases. After standing for about 12 h, the mixing solutions show precipitation except the one prepared at the molar ratio of 10.0 (Figure 1B). So it is possible to prepare dispersed PAA-Ce complex colloidal particles at the molar ratio of 10.0.

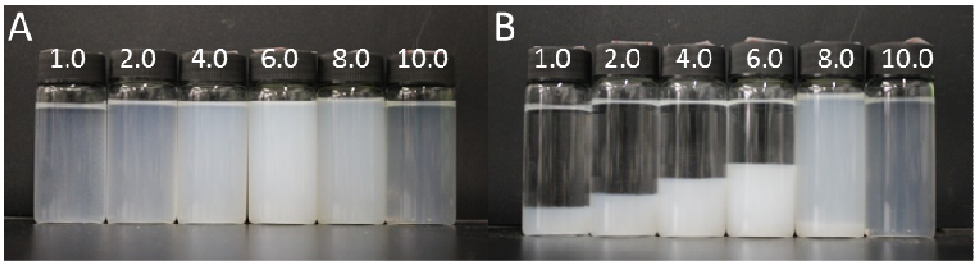

Figure 1 Photos of PAA-Ce complex solutions (Protocol 1, pH 6.0) with different molar ratios ([AA]/[Ce]: 1.0, 2.0, 4.0, 6.0, 8.0 and 10.0), (A) just mixed, (B) 12 h after mixing.

From stoichiometry aspect, a lanthanide ion (III) interacts with three COO^- group.[36, 37] At pH 6.0, the ionization degree of PAA is about 50 %.[38-40] At the molar ratio 6.0, the ionized COO^- groups are about 3 times to Ce^{3+} ions. So the mixed PAA and $CeCl_3$ solution is cloudiest. When the molar ratio is higher than 6.0, there are excessive COO^- groups available, which will make the complex particles negatively

charged. According DLVO theory, introducing electric charges on the surface of the PAA-Ce complex particles can improve the kinetic stability and prevent aggregation.[41] At the molar ratio 8.0, the precipitation becomes slow. When the molar ratio elevates to 10.0, there are more excessive charges, and the complex particles do not show sediment and are homogeneously dispersed.

At pH 6.0 and the molar ratio of 10.0, we applied three protocols to prepare PAA-Ce complex nano-particles: (1) Directly mixing PAA and Ce^{3+} solution; (2) Ce^{3+} solution is drop-wise added into PAA solution; (3) PAA solution is drop-wise added into Ce^{3+} solution. With these three protocols, the solutions show different turbidity, ranked as Protocol 3 > Protocol 1 > Protocol 2 (Figure 2). Figure 2 exhibits particle size distribution revealed by DLS. The average hydrodynamic diameters of Protocol 1 particles and Protocol 3 particles are 168 nm and 244 nm, respectively. However, the hydrodynamic diameter of Protocol 2 particles is very small, less than 10 nm. Protocol 3 produces the largest complex colloidal particles, Protocol 2 the smallest, and Protocol 1 in the middle. The zeta potentials of the complex particles were measured. The values of the complex particles prepared with Protocol 1, 2 and 3 are -8.82, -11.60 and -27.80 mV, respectively.

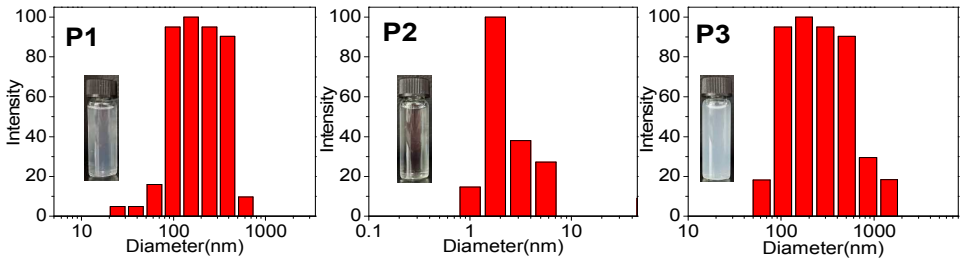

Figure 2 Particle size distributions of PAA-Ce complex colloids prepared by three different protocols: P1, P2 and P3. The inset photos are the corresponding complex solutions. ([AA]/[Ce] = 10.0, pH = 6.0).

Under Protocol 1, PAA solution and Ce^{3+} ion solution are mixed directly, and the complex particles grow spontaneously. Under Protocol 2, Ce^{3+} ion solution is drop-wise added into PAA solution. Carboxylate groups from PAA chains are

excessive all the time. When Ce^{3+} ions are added into solution, they will be captured by the PAA chains and the polymer-metal complex particles are very hard to grow big. Under Protocol 3, PAA solution is drop-wise added into Ce^{3+} ion solution. Initially there are excessive Ce^{3+} ions in the system, and hence PAA chains will be cross-linked at the beginning and the nuclei will be easily formed. As more PAA chains are added into the system, the PAA-Ce complex particles will grow up.

LbL assembly of PDDA and PAA-Ln complex colloidal particles

The PAA-Ce complex colloidal particles are prepared at pH 6.0. pH values of PDDA solution and rinsing solutions all are adjusted to 6.0 to conduct LbL assembly. The UV-Visible spectrometer monitoring demonstrated that PDDA and PAA-Ce complex colloidal particles were successfully LbL assembled (SI, Figure S1). If pH values of PAA-Ce colloidal solution and rinsing solutions are kept at 6.0 while the pH value of PDDA decreases to 2.0, the film will be very hard to fabricate (SI, Figure S2). However, when pH value of PDDA solution is elevated to 10, the film is easy to prepare. PDDA is strong cationic polyelectrolytes, and its ionization does not show dependence on pH value. The PDDA can be adsorbed on the substrate at low pH value. But if pH value is too low, the negatively charged PAA will be neutralized and the PDDA-PAA association based on electrostatic force is very difficult to happen at interface. PAA-Ce coordination in the complex colloidal particles will be interrupted when PAA is protonized. [38] So the assembly will fail when the pH values of the assembling solutions are too low. To avoid pH effect on LbL assembly, the pH values of all solutions, including assembling solutions and rinsing solutions, are fixed at pH 6.0.

The reflection spectra of the films fabricated with 20 assembling cycles are show in Figure 3. On the reflection spectra, there are some vibrational peaks which are named as Fabry-Pérot fringes.[42-44] Fabry-Pérot fringes are formed on spectra due to optical interference of the film, and can be used to estimate film thickness.[45,46] $[PDDA/(PAA@Ce)]_{20}$ films fabricated by using Protocol 1, 2 and 3 colloidal particles are 919, 784, and 1058 nm respectively. Without complexation with lanthanide ion,

PAA can directly LbL assembled with PDDA to fabricate film. However, PDDA/PAA film thickness growth is much slower that of PDDA/(PAA@Ce) film. PDDA/PAA film only grows several nanometers per assembling cycle.[3-5] The average growth per assembling cycle of PDDA/PAA@Ce film is about one-order higher than that of PDDA/PAA film.

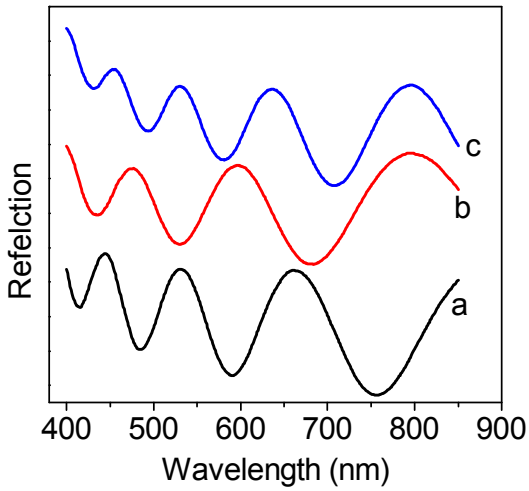

Figure 3 Reflection spectra of three $[PDDA/(PAA@Ce)]_{20}$ films which are fabricated with different PAA-Ce complex colloids particles: (a) Protocol 1 particles; (b) Protocol 2 particles; (c) Protocol 3 particles (for clarity, the spectra curves are intentionally overlaid).

The hydrodynamic diameter of Protocol 2 particles is less than 10 nm, but the resulting $[PDDA/(PAA@Ce)]_{20}$ is high as 784 nm. The hydrodynamic diameter of Protocol 3 particles is 244 nm, but the resulting $[PDDA/(PAA@Ce)]_{20}$ is only 1058 nm. The thickness contrast of the two films is not distinct like the size contrast of their building colloidal particles. QCM was applied to monitor the assembly behavior of PDDA and PAA-Ce complex particles, as shown in Figure 4. The frequency shift in QCM reflects the mass deposited on the chips. The relationship between frequency shift and mass is described as equation as below: [47]

$$\Delta m = -C\frac{\Delta f}{n} \qquad (1)$$

where Δm, Δf, C, and n are the mass increment, the frequency shift, the constant of the resonant chip and the overtone number, respectively.

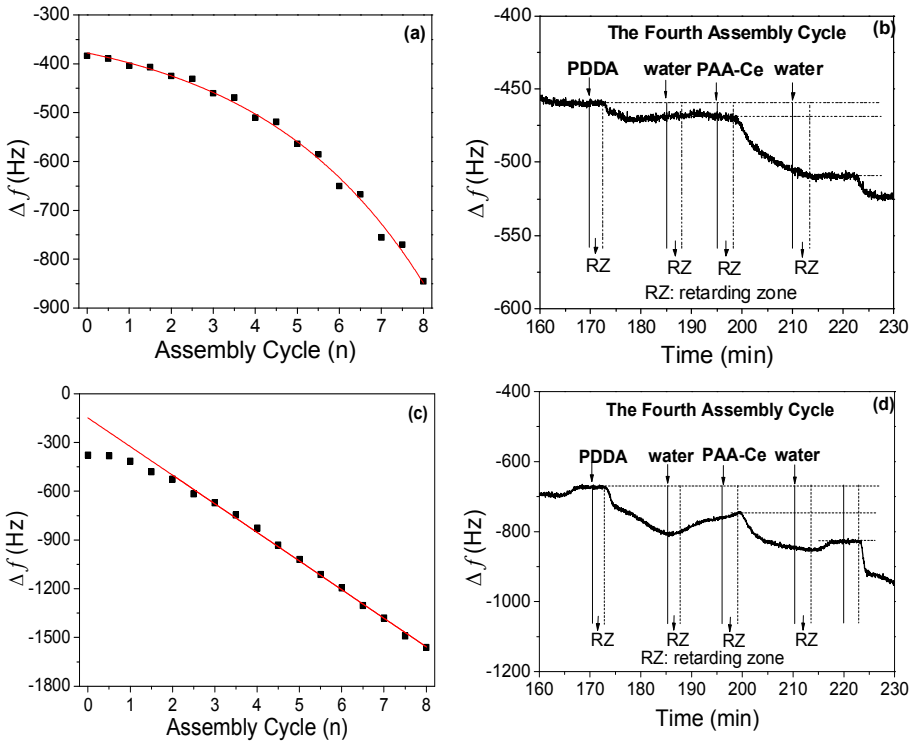

Figure 4 QCM monitoring the LbL assembly of PDDA and PAA-Ce complex colloidal particles. (a-b): LbL assembly of PDDA and Protocol 2 particles; (c-d): LbL assembly of PDDA and Protocol 3 particles; (a) and (c): frequency as a function of assemble cycle; (b) and (d): the frequency shift as a function of time in the fourth assembly cycle. (PDDA: 15 min; rinsing water: 10 min; PAA-Ce complex nanoparticle: 15 min; it took 3-4 min for the switched solution from the vial to the chamber, which was defined as retarding zone)

QCM monitoring demonstrated different assembly behavior between Protocol 2 film and Protocol 3 film. Through curve fitting, the assembly of PDDA and Protocol 2 particles shows exponential growth (Figure 4a) while that of Protocol 3 and PDDA particles shows linear growth after three assembling cycles (Figure 4c). In the assembly of PDDA and Protocol 2 particles, the weight of Protocol 2 particles deposited on the chips is higher than that of PDDA. However, in the assembly of

PDDA and Protocol 3 particles, the weight of Protocol 3 particles deposited on the chips is almost equal to that of PDDA.

The frequency shift as a function of time in the fourth assembly cycle reveals the details of the assembly. For the assembly of PDDA and Protocol 2 particles, it is very hard to observe desorption after pumping rinsing water. But for the assembly of PDDA and Protocol 3 particles, desorption is obvious after sending water into the chamber.

Protocol 2 particles are small and have low zeta-potential. LbL assembly of PDDA and Protocol 2 particles shows exponential thickness growth, indicating that diffusion and fusion of Protocol 2 particles should happen during the assembly. [48] It interprets that why the hydrodynamic diameter of Protocol 2 particles is less than 10 nm, but the resulting $[PDDA/(PAA@Ce)]_{20}$ is about 800 nm. Protocol 3 particles are big and have high zeta-potential. PDDA chains would squeeze Protocol 3 particles during the assembly process. Though the average hydrodynamic diameter of Protocol 3 particles is high as 244 nm, the resulting $[PDDA/(PAA@Ce)]_{20}$ is only about 1100 nm.

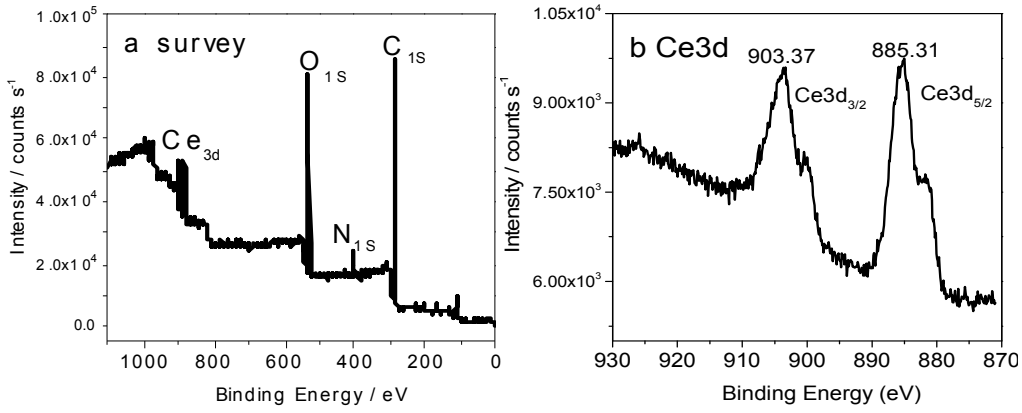

Figure 5 XPS curve of $[PDDA/(PAA@Ce)]_{20}$ thin film. (Protocol 3 particles, PDDA concentration is 0.01 mol/L).

Among three protocols, Protocol 3 is recommended to prepare PAA-Ln complex colloidal particles for LbL assembly. Protocol 3 produces the most kinetical stable particles. The LbL assembly of PDDA and Protocol 3 particles exhibits quick and stable thickness growth after several initial assembling cycles. The film made from PDDA and Protocol 3 particles was scratched off from the substrate and then was characterized with ICP-AES. Ce content in the thin film was determined to be 8.5%. XPS was utilized to illustrate that Ce^{3+} ions are bound in the film (Figure 5). The thin film shows two characteristic peaks of Ce^{3+} ions. One is Ce $3d_{5/2}$ peak at 885.31 eV and the other is Ce $3d_{3/2}$ peak at 903.37 eV. For cerium chloride ($CeCl_3$), the peaks are located at 888.30 and 908.00 eV, respectively.[49, 50] The two peaks of Ce^{3+} in the film shift to the lower energy sides, compared with those of $CeCl_3$. In the thin film, Ce^{3+} ions coordinate with carboxylate groups of PAA, which increases electron density of Ce atoms and makes binding energy decrease.

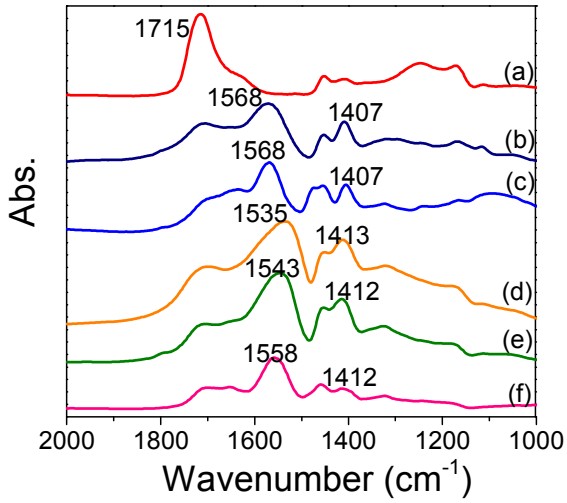

Figure 6 FT-IR spectra: (a) PAA, non-ionized; (b) PAA, freezing-dry from pH 6.0 solution, partially ionized (PAA-pH 6.0); (c) PDDA-PAA bulk complex, prepared at pH 6.0 with [AA]/[DDA] = 1.0; (d) PAA-Ce complex, pH = 6.0, [AA]/[Ce] = 1.0; (e) PAA-Ce complex, pH = 6.0, [AA]/[Ce] = 10.0; and (f) $[PDDA/(PAA@Ce)]_{20}$ thin film (pH = 6.0, [AA]/[Ce] = 10.0, PDDA = 0.01 mol/L). The spectra were intentionally overlaid for clarity.

FT-IR was applied to study the interaction between PAA and Ce^{3+} ions in the thin film (Figure 6). For the non-ionized PAA, the C=O stretching vibration of carboxylic acid group (-COOH) is located at 1715 cm^{-1}.[51] PAA is a weak polyelectrolyte, and it will ionize when the pH elevates. The pH value of the solution was adjusted to 6.0, where PAA have about 50 % ionization.[38-40] The spectrum shows that asymmetric $v_{asym}(COO^-)$ and symmetric $v_{sym}(COO^-)$ stretching vibration of COO^- are at 1568 cm^{-1} and 1407 cm^{-1}, respectively, and the separation between the asymmetric and the symmetric peak ($\Delta = v_{asym} - v_{sym}$) is 161 cm^{-1}.

For the PAA-Ce complex prepared at the molar ratio ([AA]/[Ce]) 1.0, the asymmetric and the symmetric stretching vibration peaks of carboxylate are located at 1535 and 1413 cm^{-1} respectively. The separation is 122 cm^{-1}. For the PAA-Ce complex prepared at the molar ratio ([AA]/[Ce]) 10.0, the asymmetric and the symmetric vibration are at 1545 cm^{-1} and 1412 cm^{-1}, respectively. The separation is 133 cm^{-1}, larger than that prepared at the molar ratio of 1.0. Compared with PAA at pH 6.0, PAA-Ce bulk complex shows the small separation of asymmetric and symmetric vibration peaks. The separation between the $v_{asym}(COO^-)$ and $v_{sym}(COO^-)$ can reflect the coordination mode between carboxylate and Ce^{3+} ion.[52] The coordination mode of $-COO^-$ and Ce^{3+} ion in the complex was suggested as chelating mode.[37, 38]

At the molar ratio of 1.0, Ce^{3+} ions are stoichiometrically excessive and all carboxylate groups will be involved in coordination. However at the mole ratio of 10.0, carboxylate groups are abundant, and some of them do not join the coordination. So the PAA-Ce complex prepared at the molar ratio 10.0 shows the bigger separation of carboxylate than that synthesized at the molar ratio 1.0.

PAA is a polyanion while PDDA is a polycation. PAA and PDDA can form inter-polymer complex. For the PDDA-PAA complex, asymmetric and symmetric vibrations of carboxylate are similar to that of the PAA sample at pH 6.0. It means that electrostatic interaction of PDDA and PAA does not reduce the separation between asymmetric and symmetric vibration peak of carboxylate.

For [PDDA/(PAA@Ce)]$_{20}$ film, the asymmetric vibration of carboxylate is located at 1558 cm^{-1} and the symmetric vibration is at 1411 cm^{-1}, and the separation is 147 cm^{-1}. The separation of carboxylate in [PDDA/(PAA@Ce)]$_{20}$ film is smaller than that of PAA (PAA-pH 6.0) and PDDA/PAA complex but bigger than that of the PAA-Ce complex particles. It indicates that during the LbL assembly of PDDA and PAA-Ce complex particles, the electrostatic interaction of PDDA-PAA has competition with coordination of coordination of PAA-Ce. The coordination of PAA-Ce in the LbL assembled film becomes weak, compared with that in the PAA-Ce complex particles.

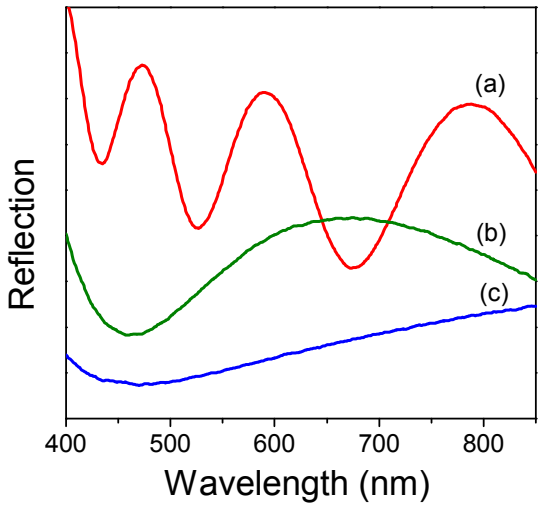

Figure 7 The reflection spectra of [PDDA/(PAA@Ce)]$_{20}$ films prepared with different PDDA concentration: (a) 0.01 mol/L; (b) 0.05 mol/L; and (c) 0.10 mol/L. PAA-Ce colloidal particles were prepared through Protocol 3.

To further demonstrate the competition between electrostatic interaction of PDDA-PAA and coordination of PAA-Ce, the concentration of PDDA solution was increased to perform LbL assembly. The reflection spectra of the films prepared with different concentration PDDA solutions are shown in Figure 7. As the PDDA concentration increases, the Fabry-Perót fringes on the spectra will gradually disappear, indicating the film thickness reduction. When PDDA is at the concentration

of 0.01 mol/L, the film thickness is more than 1000 nm. However at the concentration of 0.05 and 0.10 mol/L, the film thickness deceases to 232 and 71 nm, respectively. Also, as the concentration increased, the roughness of the corresponded thin film shows also decrease (SI, Figure S3). During the assembly, PDDA chains will squeeze the complex particles. Increasing the concentration of PDDA, more PDDA chains will diffuse to the film from the solution. So the squeezing effect is manifested and the film thickness shows great reduction.

The lanthanide ions, such as Ce^{3+}, Nd^{3+}, Sm^{3+}, Eu^{3+}, Tb^{3+}, Dy^{3+}, Er^{3+}, and Yb^{3+} show fluorescent. [53] The fluorescence property of $[PDDA/(PAA@Ce)]_{20}$ film was investigated. Under the UV light (254 nm) irradiation, the film shows tint blue color (Figure 8a). $[PDDA/(PAA@Ce)]_{20}$ film shows fluorescent excitation peak at 260 nm, which is ascribed to the 4f→5d transition of Ce^{3+} ions. Under excitation at 260 nm, the fluorescent emission peak is located at 357 nm.[54] Compared with Ce^{3+} ion in the solution, the excitation and the emission peaks show several nanometers red shift, which is due to the coordination with PAA.

Other lanthanide ions, Eu^{3+} and Tb^{3+}, were prepared into complex colloidal particles with PAA through Protocol 3 like Ce^{3+} and then LbL assembled with PDDA to fabricate films. The fluorescent spectra of $[PDDA/(PAA@Eu)]_{20}$ and $[PDDA/(PAA@Tb)]_{20}$ were shown in Figure 8b and Figure 8c, respectively.

The excitation spectrum of $[PDDA/(PAA@Eu)]_{20}$ film, recorded by monitoring $^5D_0 \rightarrow {}^7F_2$ transition at 617 nm, consists of several characteristic peaks of the Eu^{3+} ions. The sharp bands at 394 and 466 nm correspond to *f-f* characteristic transitions, from the ground $^7F_0$ state to $^5L_6$ and $^7F_2$ multiple terms, respectively.[55, 56] The emission spectrum, under excitation at 395 nm, is dominated by the $^5D_0 \rightarrow {}^7F_2$ transition at 617 nm, which makes the film show red color under the UV light. The intensity ratio of $^5D_0 \rightarrow {}^7F_1$ (595 nm) transition and $^5D_0 \rightarrow {}^7F_2$ (617 nm) transition can provide some structural information about coordination. If $^5D_0 \rightarrow {}^7F_1$ (595 nm) transition stronger than $^5D_0 \rightarrow {}^7F_2$ (617 nm), Eu^{3+} ion will be located at the sites of inversion symmetry. Otherwise, the coordination of Eu^{3+} takes non-inversion symmetry. In $EuCl_3$ solution, the intensity of peak at 592 nm is stronger than that of peak at 617 nm. Eu^{3+} ions

coordinate with water under inversion symmetry. In the film the intensity of peak at 595 nm is lower than that of peak at 617 nm, indicating that Eu^{3+} ion is not in inversion symmetry. Eu^{3+} ion not only coordinates with carboxylate group but also interacts with water in the film.

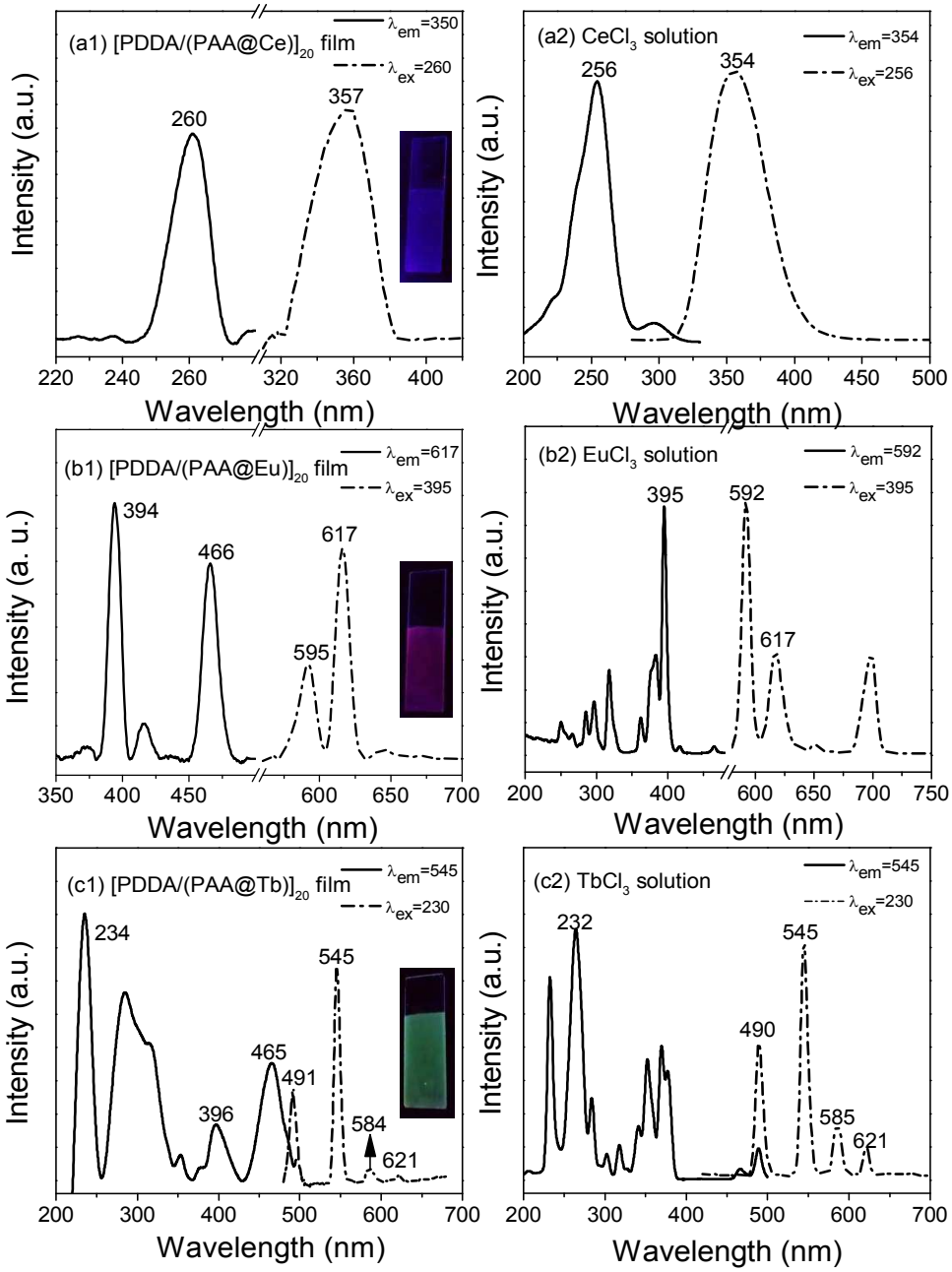

Figure 8 Excitation spectra and emission spectra of the $[PDDA/(PAA@Ce)]_{20}$, $[PDDA/(PAA@Eu)]_{20}$, and $[PDDA/(PAA@Tb)]_{20}$ films and the corresponding $LnCl_3$

solutions. (PAA-Ce, PAA-Eu and PAA-Tb are all prepared with Protocol 3 and PDDA concentration is 0.01 mol/L)

For $[PDDA/(PAA@Tb)]_{20}$ film, the excitation spectrum exhibits several bands in the range from 200 to 500 nm. The strong band at about 230 nm is due to the f-f transition of the Tb^{3+} ions, from $^7F_5 \rightarrow {}^5G_6$. The emission spectrum consists of four main characteristic peak of Tb^{3+} ions, i.e., $^5D_4 \rightarrow {}^7F_6$ (491 nm), $^5D_4 \rightarrow {}^7F_5$ (545 nm), $^5D_4 \rightarrow {}^7F_4$ (584 nm), $^5D_4 \rightarrow {}^7F_3$ (621 nm).[57] Among these emission peaks, the green emission at 545 nm ($^5D_4 \rightarrow {}^7F_5$) is the strongest one.

The post-treatment of $[PDDA/(PAA@Ce)]_{20}$ film

$[PDDA/(PAA@Ce)]_{20}$ films were incubated in PDDA solution and $CeCl_3$ solution, separately. After incubation, the film exhibited different cloudiness as shown in the inset of Figure 9. After incubation in PDDA solution the film became transparent and the film thickness showed 20 % reduction (SI, Figure S4), and at the same time we can detect Ce^{3+} in PDDA solution through fluorescence measurement (SI, Figure S5). After incubation in $CeCl_3$ solution the film became even cloudy and thickness exhibited 13 % increment (SI, Figure S6).

After incubation, the films were characterized with FT-IR. Incubation in PDDA solution makes the separation between symmetric vibration and asymmetric vibration enlarge, which demonstrates the PDDA-PAA association based on electrostatic interaction in the thin film is strengthened. However, incubation in $CeCl_3$ solution induces the separation to become narrow, indicating the association of PAA-Ce based on coordination in the film intensifies.

In $[PDDA/(PAA@Ce)]_{20}$ film, PDDA and PAA have electrostatic interaction while PAA and Ce^{3+} ion have coordination. There is a dynamic equilibrium. Incubation in PDDA solution or $CeCl_3$ solution will make the equilibrium shift. Putting the film into PDDA solution, PDDA chains will diffuse into the film, and the PDDA-PAA association in the film based on electrostatic interaction will be strengthened whereas the PAA-Ce association in the film based on coordination will

become weak. Dipping into $CeCl_3$ solution, Ce^{3+} ions will penetrate into the film, and the PAA-Ce association will be strengthened while the PDDA-PAA association will be weakened. Metals and organic polymers have big refractive index contrast. As more Ce^{3+} ions enter into the film to complex with PDDA, light scattering effect will intensify and therefore the film will become much cloudy.

$[PDDA/(PAA@Ce)]_{20}$ films were also immersed into sodium chloride (NaCl) solutions (SI, Figure S7). After immersion in NaCl solution, the film becomes thin. After dipping in 0.5 M NaCl for 24 h, the film showed 80 % thickness reduction. However, after immersion in 0.7 M NaCl solution for 24 h, the film was almost dissolved. The salt shields the electrostatic interaction between PDDA and PAA and also affects the coordination between PAA and cerium ion. So the strong ionic strength will destroy the interaction equilibrium in $[PDDA/(PAA@Ce)]_{20}$ film and hence the film will disintegrate.

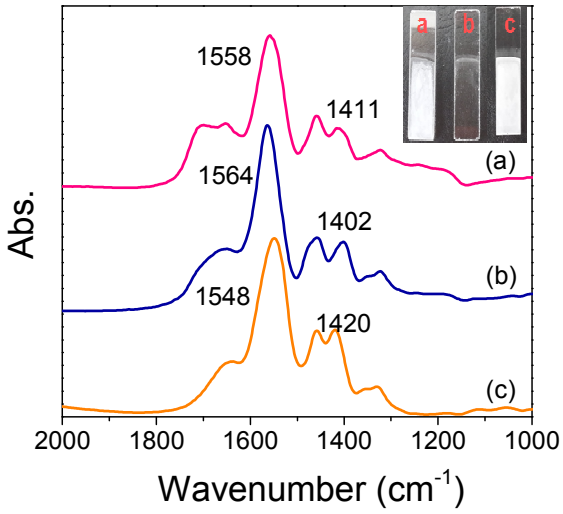

Figure 9 Photographs and IR spectra of $[PDDA/(PAA@Ce)]_{20}$ films: (a) the film as prepared; (b) the film was incubated in 0.01 mol/L PDDA solution for 24 h; (c) the film was incubated into 0.01 mol/L $CeCl_3$ solution for 24 h. The insets are corresponding pictures.

Conclusions

The homogenously dispersed PAA-Ce complex colloidal particles can be prepared at pH 6.0 and molar ratio 10.0. PAA-Ce colloidal particle size can be adjusted through different mixing protocols. PDDA and PAA-Ce colloidal particles can be LbL assembled to prepare the composite film. $[PDDA/(PAA@Ce)]_{20}$ film grows much quicker than $[PDDA/PAA]_{20}$ film does. The incorporated lanthanide ions can make the film exhibit fluorescence under UV-irradiation.

The LbL assembly of PDDA and PAA-Ln complex colloidal particles is a dynamic process. PAA-Ln complex colloidal particles will be squeezed or diffuse/fuse during LbL assembly depending on their size, structure and surface properties.

PDDA and Ln^{3+} have competition to interaction with PAA and hence there is equilibrium in PDDA/(PAA@Ln) film. Strong ionic strength can destroy the equilibrium in PDDA/(PAA@Ln) film and make the film dissolve.

Acknowledgements

S. Y. gratefully acknowledges the support from National Natural Science Foundation of China (NSFC, Grant No. 51373032), Innovation Program of Shanghai Municipal Education Commission, Fundamental Research Funds for the Central University and DHU Distinguished Young Professor Program.

References

1 G. Decher and J. D. Hong, *Makromol. Chem. Macromol. Symp.*, 1991, **46**, 321.

2 G. Decher and J. D. Hong, *Ber. Bunsenges. Phys. Chem.*, 1991, **95**, 1430.

3 G. Decher, J. D. Hong and J. Schmitt, *Thin Solid Films*, 1992, **210**, 831.

4 G. Decher, *Science*, 1997, **277**, 1232.

5 P. Bertrand, A. Jonas, A. Laschewsky and R. Legras, *Macromol. Rapid Commun.*, 2000, **21**, 319.

6 P. Lavalle, J. C. Voegel, D. Vautier, B. Senger, P. Schaaf and V. Ball, *Adv. Mater.*, 2011, **23**, 1191.

7 A. Katsuhiko, J. P. Hill and Q. Ji, *Phys. Chem. Chem. Phys.*, 2007, **9**, 2319.

8 S. Yang, S. Ma, C. Wang, J. Xu and M. Zhu, *Aust. J. Chem.*, 2014, **67**, 11.

9 S. Ma, Q. Yuan, X. Zhang, S. Yang and J. Xu, *Colloids Surf. A-Physicochem. Eng. Asp.*, 2015, **471**, 11.

10 Y. Lvov, K. Ariga, I. Ichinose and T. Kunitake, *J. Am. Chem. Soc.,* 1995, **117**, 6117.

11 M. H. M. A. Shibraen, C. Wang, H. Yagoub, Q. Yuan, S. Yang and J. Xu, *RSC. Advances*, 2014, **4**, 55459.

12 B. Wu, C. Li, H. Yang, G. Liu and G. Zhang, *J. Phys. Chem. B*, 2012, **116**, 3106.

13 F. Huo, H. Xu, L. Zhang, Y. Fu, Z. Wang and X. Zhang, *Chem. Commun.*, 2003, 874.

14 S. Srivastava and N. A. Kotov, *Acc. Chem. Res.*, 2008, **41**, 1831.

15 N. F. Steinmetz, G. Calder, G. P. Lomonossoff and D. J. Evans, *Langmuir*, 2006, **22**, 10032.

16 J. Sun, X. Liu and J. Shen, in *Mutilayer thin film*, ed. G. Decher and J. B. Schlenoff, Wiley-VCH Verlag & Co. KGaA , Germany, 2nd edition, chapter 7.

17 Y. Li, X. Wang and J. Sun, *Chem. Soc. Rev.*, 2012, **41**, 5998.

18 Y. Zhang, W. Cao and J. Xu, *J. Colloid. Interf. Sci.*, 2002, **249**, 91.

19 Q. Zhao, J. Qian, Q. An and B. Du, *J. Mater. Chem.*, 2009, **19**, 8448.

20 E. Tsuchida, K. Abe, *Adv. Polym. Sci.*, 1982, **45**, 1.

21 Y. Li, L. Li and J. Sun, *Angew. Chem. Int. Ed.*, 2010, **49**, 6129.

22 Y. Li, S. Chen, M. Wu and J. Sun, *Adv. Mater.*, 2014, **26**, 3344.

23 M. Cui, W. S. Ng, X. Wang, P. Darmawan and P. S. Lee, *Adv. Funct. Mater.*, 2015, **25**, 401.

24 L. Zhang and J. Sun, *Chem. Commun*., 2009, 3901.

25 X. Liu, B. Dai, L. Zhou and J. Sun, *J. Mater. Chem*., 2009, **19**, 497.

26 X. Liu, L. Zhou, W. Geng and J. Sun, *Langmuir*, 2008, **24**, 12986.

27 F. Ciardelli, E. Tsuchida and D. Wöhrle, *Macromolecule-Metal Complexes*, Springer-Verlag, Germany, 1989.

28 X. Huang and N. S. Zacharia, *ACS. Macro. Lett.*, 2014, **3**, 1092.

29 X. Huang, A. B. Schubert, J. D. Chrisman and N. S. Zacharia, *Langmuir*, 2013, **29**,

12959.

30 A. M. Balachandra, J. Dai and M. L. Bruening, *Macromolecules*, 2002, **35**, 3171.

31 K. C. Krogman, K. F. Lyon and P. T. Hammond, *J. Phys. Chem. B*, 2008, **112**, 14453.

32 P. Schuetz and F. Caruso, *Adv. Funct. Mater.*, 2003, **13**, 929.

33 J. Dai and M. L. Bruening, *Nano. Lett.*, 2002, **2**, 497.

34 K. Binnemans, *Chem. Rev*. 2009, **109**, 4283.

35 Y. Cui, Y. Yue, G. Qian and B. Chen, *Chem. Rev*. 2012, **112**, 1126.

36 B. L. Rivas, E. D. Pereira and I. Moreno-Villoslada, *Prog. Polym. Sci*., 2003, **28**, 173.

37 F. Q. Huang, Y. Zheng and Y. Yang, *J. Appl. Polym. Sci.*, 2007, **103**, 351.

38 X. Qi, Z. Wang, S. Ma, L. Wu, S. Yang and J. Xu, *Polymer*, 2014, **55**, 1183.

39 S. Yang, Y. Zhang, X. Zhang and J. Xu. *Soft Matter*, 2007, **3**, 463.

40 J. Choi and M. F. Rubner, *Macromolecules*, 2005, **38**, 116.

41 P. C. Hiemenz and R. Rajagopalan, in *Principles of Colloidal and Surface Chemistry*, 3rd edition, Chapter 1,CRC, Taylor & Francis Group, Florida, 1997.

42 S. Yang, Y. Zhang, X. Zhang, Y. Guan, J. Xu and X. Zhang, *Chem. Phys. Chem.*, 2007, **8**, 418.

43 J. Ma, S. Yang, Y. Li, X. Xu and J. Xu, *Soft Matter*, 2011, **7**, 9435.

44 S. Yang, Y. Zhang, L. Wang, S. Hong, J. Xu, Y. Chen and C. Li, *Langmuir*, 2006, **22**, 338.

45 S. Yang, S. Tan, Y. Zhang, J. Xu and X. Zhang, *Thin Solid Films*, 2008, **516**, 4018.

46 S. Yang, Y. Zhang, Y. Guan, S. Tan, X. Zhang, S. Cheng and J. Xu, *Soft Matter*, 2006, **2**, 699.

47 G. Z. Sauerbrey , *Phys.* 1959 , **15** , 206 .

48 C. Picart, J. Mutterer, L. Richert, Y. Luo, G. D. Prestwich, P. Schaaf, J.-C. Voegel, and P. Lavalle, *Proc. Natl. Acad. Sci. U. S. A.* 2002, **99**, 12531

49 R. Martínez-Martínez, M. Garacía-Hipólito, L. Huerta, J. Rickards, U. Caliño, and C. Falcony, *Thin Solid Films*, 2006, **515**, 607.

50 J. F, Moulder, W. F. Stickle, P. E. Sobol and K. D. Bomben, *Handbook of X-ray Photoelectron Spectroscopy*, Perkin-Elmer Corporation Physical Electronics Division, Eden Prairie, Minnesota, 1992.

51 J. Dong, Y. Ozaki and K. Nakashima, *Macromolecules*, 1997, **30**, 1111.

52 G. B. Deacon and R. J. Phillips, *Coordin Chem Rev*, 1980, **33**, 227.

53 C. Huang, *Rare Earth Coordination Chemistry: Fundamentals and Applications*, John Wiley & Sons (Asia) Pte Ltd, Singapore, 2010.

54 J. He, G. Ren, Y. Mao and L. Xiang, *Optics Communi.*, 2014, **323**, 174.

55 H. Yang and Y. Kim, *J. Lumin.*, 2008, **128**, 1570.

56 X. Zhou, K. Zhou, Z. Wang and S. Yang, *Z. Anorg. Allg. Chem.*, 2013, **639**, 121.

57 Y. Huang, H. You, G. Jia, Y. Song, Y. Zheng, M. Yang, K. Liu and N. Guo, *J. Phys. Chem. C*, 2010, **114**, 18051.